Journal of Integrative Neuroscience

J. Integr. Neurosci. **2026**; 25(5): 49065
https://doi.org/10.31083/JIN49065

Original Research

Tea Polyphenols Protect the Blood–Brain Barrier Structure in the Hippocampus of Early Diabetic Mice by Inhibiting the AGEs–RAGE Pathway

Zhiyong Xu[1,2], Yan Liu[3], Yan Yu[1,2,*]

[1]College of Animal Science and Veterinary Medicine, Henan Institute of Science and Technology, 453003 Xinxiang, Henan, China
[2]Henan International Joint Laboratory of Animal Health Breeding and Disease Prevention and Control, Henan Institute of Science and Technology, 453003 Xinxiang, Henan, China
[3]Emergency Department, The 83rd Army Group Hospital of the Chinese People's Liberation Army, 453003 Xinxiang, Henan, China
*Correspondence: yymtt03@163.com (Yan Yu)
Academic Editor: Hajime Hirase
Submitted: 13 December 2025 Revised: 9 February 2026 Accepted: 12 February 2026 Published: 12 May 2026

Abstract

Background: Diabetic encephalopathy is a prevalent complication of diabetes mellitus, which is primarily characterized by hippocampal injury and blood-brain barrier (BBB) dysfunction. This study investigates the neuroprotective effect of tea polyphenols (TP) on hippocampal tissue in early-stage diabetic mice. **Methods**: Sixty BALB/c mice were randomly assigned to the control group (C), the diabetes group (T0), and the TP-treated group (T1). After successful model induction, mice in group T1 received TP intragastrically (100 mg/kg/d). Hematoxylin and eosin (H&E), toluidine blue, and Hoechst 33342 staining, combined with polymerase chain reaction (PCR) and enzyme-linked immunosorbent assay (ELISA), were used to assess the effects of TP on hippocampal histology, inflammation and oxidative stress, the advanced glycation end products (AGEs) – Receptor for Advanced Glycation End products (RAGE) pathway, and the expression of key proteins associated with the BBB. **Results**: The contents of AGEs, RAGE, NF-κB, P-glycoprotein (P38), and oxidative stress factors in group T1 were lower than those in group T0 at 7, 14, and 21 days ($p < 0.05$). At the same time points, the mRNA expression levels of inflammatory factors in group T1 were lower than those in group T0 ($p < 0.05$). Moreover, compared with group T0, both P-glycoprotein (P-gp) protein expression and glucose transporters (*Glut1*) mRNA expression increased in group T1 ($p < 0.05$). The mRNA expression levels of key BBB-related molecules in group T1 also increased to varying degrees ($p < 0.05$). Histopathological analysis showed marked improvement in the hippocampal architecture of group T1 compared with group T0. Moreover, the expression levels of P38, NF-κB, *IL-6*, *TNF-*α, ROS, and *Glut1* were significantly or highly significantly positively correlated with RAGE protein levels ($p < 0.05$ or $p < 0.01$). **Conclusions**: TP enhanced BBB structural integrity by inhibiting the AGEs–RAGE pathway, thereby attenuating hippocampal tissue damage.

Keywords: tea polyphenols; hippocampus; blood–brain barrier; AGEs; RAGE

1. Introduction

Diabetes mellitus (DM) is a chronic metabolic disease and is now one of the major threats to human health. By 2045, an estimated 693 million people worldwide are projected to have diabetes. As blood glucose levels rise, cellular glucose tolerance reaches a threshold. Excessive hyperglycaemia damages neural tissues and disrupts microvascular integrity by triggering oxidative stress, activating inflammatory responses, and initiating coagulation mechanisms, leading to multisystem injury and complications [1]. Current research indicates that most diabetic patients exhibit structural damage to the hippocampus and the blood–brain barrier (BBB), leading to neurocognitive impairment and neurological disorders [2].

The BBB is a highly selective semipermeable structural and functional barrier formed by continuous capillary endothelial cells (ECs) connected through tight junctions (TJs). It separates the central nervous system (CNS) from peripheral blood circulation and prevents potentially harmful circulating substances from entering the brain [3]. As a critical structural component of the BBB, dysregulation of TJ proteins contributes to BBB disruption. When TJs are damaged, the permeability of the BBB increases, immune cell extravasation rises, and molecular and ion flux across the barrier becomes dysregulated. TJs are anchored to the actin cytoskeleton through transmembrane proteins—including claudins, occludin, and junctional adhesion molecules (JAMs)—which interact with cytoplasmic scaffolding proteins of the zonula occludens (ZO) family [4]. Claudins—particularly claudin-5 and claudin-3, form the primary seal of TJs by homophilic interactions with identical claudins on adjacent ECs and determine paracellular permeability and charge selectivity [5,6]. Occludin is highly enriched in CNS ECs and is a major transmembrane protein of TJs. Its carboxyl terminus binds the PDZ domain of ZO, influencing BBB integrity, permeability, and intracellular signalling [7]. JAM is a cell adhesion molecule that enhances endothelial barrier function, regu-

lates leukocyte adhesion, and modulates paracellular permeability. As a cytoskeletal linker, the ZO complex assists claudin, occludin, and JAM in anchoring to the cytoskeleton [8]. A previous study showed that several key BBB proteins in the hippocampus of early DM mice are altered [9]. Moreover, P-glycoprotein (P-gp) is an ATP-binding cassette (ABC) transporter with efflux activity in brain ECs. Under hyperglycaemic conditions, immortalised human brain microvascular ECs significantly downregulated ZO-1 within 24 h and showed upregulation of P-gp membrane expression [10]. Glucose transporters (Glut) are a key family of membrane proteins that regulate intracellular and extracellular glucose balance, with Glut1 being essential for glucose metabolism. Deficiency of Glut1 disrupts glucose transport across the BBB, leading to persistent brain energy insufficiency and neurological disease. Serum levels of major inflammatory markers in type 2 diabetes mellitus (T2DM), including IL-1β, IL-6, TNF-α, and C-reactive protein (CRP), increase significantly. MDA is elevated, whereas SOD activity is reduced compared with healthy controls [11].

Advanced glycation end products (AGEs) are generated through excessive binding of sugars to proteins. They are widely distributed in tissues and exert pathophysiological effects primarily by binding to the receptor for advanced glycation end products (RAGE) on cell membranes. RAGE is a polyligand member of the immunoglobulin superfamily. AGE–RAGE interaction activates the AGEs–RAGE signalling cascade and downstream pathways, including P38 mitogen-activated protein kinase (P38 MAPK), nuclear factor-κB (NF-κB), and phosphatidylinositol 3-kinase. These pathways promote inflammation and oxidative stress, contributing to diabetic complications. NF-κB regulates the expression and release of inflammatory factors and can exacerbate diabetes [12]. Interaction between RAGE and Aβ reduces TJ protein expression, increases BBB permeability, and accelerates capillary leakage [13]. Thus, inhibiting activation of the AGEs–RAGE pathway and its downstream effectors is an effective strategy to prevent diabetes progression. Although several AGE inhibitors have been identified, including aminoguanidine, OPB-9195, ALT-946, LR-90, and pyridoxamine, their clinical use is limited by adverse effects. Therefore, medicinal components that reduce AGEs and RAGE expression have become a major focus of research.

Tea polyphenols (TP) are natural antioxidants that inhibit the oxidation of unsaturated fatty acids and exert anti-inflammatory, lipid-lowering, glucose-lowering, and cardiocerebrovascular protective effects. Epigallocatechin gallate (EGCG), a principal component of TP, increases the expression of survival markers in adipose-derived stem cells isolated from diabetic rats under high-glucose conditions and decreases serum oxidative stress [14]. Green tea also prevents hippocampal neuronal apoptosis in diabetic rats by inhibiting the Jun N-terminal kinase/Myosin light-chain kinase (JNK/MLCK) pathway and improves cognitive function [15].

Current evidence indicates that AGEs and RAGE are markedly elevated in the brain tissues of diabetic mice [16]. AGEs accumulate through non-enzymatic glycosylation and, upon binding RAGE, activate pathways such as JNK/P38 MAPK, contributing to progressive neural damage [17,18] and offering a potential molecular target for intervention. Although TP has shown beneficial effects in diabetic neuropathy, its mechanism remains incompletely described. In particular, whether TP modulates the hippocampal structure in diabetic mice by regulating the AGEs–RAGE signalling pathway has not been systematically examined. Therefore, this study used hematoxylin and eosin (H&E), toluidine blue, and Hoechst 33342 staining, combined with polymerase chain reaction (PCR) and enzyme-linked immunosorbent assay (ELISA), to assess the effects of TP on key proteins in the AGEs–RAGE pathway, inflammation and oxidative stress, and BBB-related structural proteins in the hippocampus of early-stage diabetic mice. These findings provide a mechanistic foundation for the protective role of TP in neurological dysfunction in early-stage diabetes.

2. Materials and Methods

2.1 Construction of a Diabetes Model

Sixty BALB/c mice were housed at 25 $\pm$ 3 °C and 50–70% humidity under a light–dark cycle with free access to food and water. After three days, they were randomly assigned to the control group (C, n = 20), the diabetes model group (T0, n = 20), and the TP (Batch No. 040508, Wuhan Ya Fa Biotechnology Company, Wuhan, Hubei, China)-treated group (T1, n = 20). Except for group C, all mice received a high-fat diet (mouse feed mixed with lard) and high-sugar drinking water (50% glucose solution) for two weeks. They were then intraperitoneally injected with Streptozotocin (STZ, Product Number: S0130-100. Sigma-Aldrich, Burlington, MA, USA)–citric acid buffer (45 mg/kg) for two consecutive days. One week later, fasting blood glucose (FBG) was measured.

The criteria for successful establishment of a diabetic mouse model are as follows: (1) fasting blood glucose (FBG) concentration exceeding 11.1 mmol/L; and (2) manifestation of classic diabetic symptoms—including polydipsia, polyphagia, and polyuria. These criteria are uniformly evaluated on the 7th day after the intervention of high-sugar and high-fat diet feeding combined with STZ intraperitoneal injection. Prior to assessment, mice are fasted for 12–16 hours with unrestricted access to water. Model establishment is deemed successful if both criteria are concurrently fulfilled.

After successful modelling, all mice were provided normal feed and water. Mice in group T1 received TP solution by gavage (100 mg/kg/d, once daily), whereas groups C and T0 received the same dose of saline. Administra-

tion continued for 21 days. FBG was measured every 3–4 days. All animal procedures were approved by the Scientific Ethics Committee of Henan Institute of Science (License No. LLSC2021034).

2.2 Measurement of Body Weight

The initial body weight of mice was recorded before modelling. Body weight in each group was measured on days 1, 7, 14 and 21, and average values were calculated to document weight changes.

2.3 Measurement of Water Intake

Water intake on the first day of the experiment was recorded. Daily water intake was then measured at a fixed time. On days 7, 14 and 21, the average weekly water intake per mouse was recorded. The calculation formula was:

Average water intake (g/d) = [Total water intake in a week (g) – Remaining water weight on the recorded day (g)] / {[(Time) (d)] × [Number of mice per cage (only)]}.

2.4 Observation of Bedding

During the final week of the experiment, bedding wetness was recorded after one day under identical bedding conditions and the same number of mice per cage.

2.5 Tissue Sampling

On days 1, 7, 14 and 21, five mice were randomly selected from groups C, T0 and T1, batch execution without repeated measurement. Mice were euthanized with 1% pentobarbital sodium (Cat. No: P3761, Sigma-Aldrich, St. Louis, MO, USA) (40 mg/kg), and hippocampal CA1 region tissues were collected. Half of each sample was fixed in 4% paraformaldehyde (PFA) (Cat. No: MM1504, Shanghai Maokang Biotechnology Co., Ltd., Shanghai, China) for paraffin embedding and H&E, toluidine blue (Cat. No: 2883914, Shanghai Macklin Biochemical Co., Ltd., Shanghai, China), and Hoechst 33342 (Cat. No: AR0039, Wuhan Boster Biological Technology Co., Ltd., Wuhan, Hubei, China) staining. The remaining tissue was stored at –80 °C for PCR and ELISA analysis.

2.6 Paraffin Sections and Staining

Hippocampal tissue fixed in 4% PFA for 48 h was rinsed in running water, dehydrated through graded ethanol, cleared in xylene, infiltrated with wax, embedded, and sectioned at 5 µm thickness. Sections were stained with H&E, toluidine blue, and Hoechst 33342 (Boster), and observed under a 400× optical microscope (ECLIPSE Ci-L, Nikon, Tokyo, Japan).

2.7 Statistics of Neuronal Swelling Index

For each group, the number of neurons with nuclear swelling per 100 neurons in the CA1 region was counted. The neuronal swelling index (%) was calculated as: (number of swollen neurons/total number of neurons) × 100.

2.8 Statistics of Congestive Vascular Index

In the CA1 region, the number of congested vessels per 30 vessels examined was recorded. The congestive vascular index (%) was calculated as: (number of congestive vessels/total number of vessels) × 100.

2.9 Statistics of Gray Values of Nissl Substance

Images of CA1 neurons were captured at 1000× magnification. Images were analysed in Image-Pro Plus7.0 (Media Cybernetics, Inc., Rockville, MD, USA). Regions from comparable locations were selected, and grey values were measured. Higher grey values indicated lower Nissl substance content.

2.10 Statistics of Apoptosis Index

The number of apoptotic cells per 100 cells in the CA1 region was counted, including ECs, neurons, glial cells, and other cell types. The apoptosis index (%) was calculated as: (number of apoptotic cells / total number of cells) × 100.

2.11 PCR Technology

Total RNA was extracted from hippocampal tissues of groups C, T0 and T1 on Days 1, 7, 14 and 21, following the manufacturer's instructions. RNA purity and concentration were measured, and 1 µg of total RNA was reverse transcribed into 20 µL cDNA. Real-time PCR was performed, and the mRNA expression levels of *ZO-1*, *JAM-3*, *ZO-3*, *claudin-5*, *claudin-3*, *occludin*, *TNF-*α, *IL-6*, *IL-1*β and *Glut1* were quantified. Relative expression levels were calculated using the $2^{-\Delta\Delta Ct}$ method. Primer sequences are shown in Table 1.

2.12 Enzyme-Linked Immunosorbent Assay (ELISA)

Cryopreserved hippocampal tissue was homogenised in pre-cooled PBS and centrifuged at 1000 ×g for 10 min at 4 °C. The supernatant was collected. Phosphorylated P38 protein was measured using a mouse phosphorylated P38 ELISA kit (ZK-5246, Shanghai ZhenKe Biological Technology Co., Ltd., Shanghai, China). Phosphorylated P65 was measured using a phosphorylated P65 ELISA kit (EY-01M8419, Shanghai Yiyan Biotechnology Co., Ltd., Shanghai, China). MDA levels were assessed using a mouse MDA assay kit (ZK-4654, Shanghai ZhenKe Biological Technology Co., Ltd.). ROS was measured using a reactive oxygen species (ROS) ELISA kit (EY-(Ela)-0372, Shanghai Yiyan Biotechnology Co., Ltd.). AGEs and RAGE protein levels were measured using mouse AGEs (ZK-4500) and RAGE (ZK-5226) ELISA kits (Shanghai ZhenKe Biological Technology Co., Ltd. Shanghai, China). P-gp was measured using a mouse P-gp ELISA kit (EY-01M8338, Shanghai Yiyan Biotechnology Co., Ltd.). Absorbance was read at 450 nm using a microplate reader (Multiskan FC, Thermo Fisher Scientific, Waltham, MA, USA), and protein concentrations were calculated according to the manufacturer's instructions.

Table 1. Primers for qPCR.

	Forward primer (5′-3′)	Reverse primer (3′-5′)
β-actin	TATGCTCTCCCTCACGCCATCC	GTCACGCACGATTTCCCTCTCAG
Claudin-3	TGGCGGCTCTGCTCACCTTAG	GGGCACCAACGGGTTATAGAAATCC
Claudin-5	TGCCTTCCTGGACCACAACATC	GCCAGCACAGATTCATACACCTTG
Occludin	TGGCTATGGAGGCGGCTATGG	ACTAAGGAAGCGATGAAGCAGAAGG
ZO-1	AACCCGAAACTGATGCTGTGGATAG	CGCCCTTGGAATGTATGTGGAGAG
ZO-3	ACCACAGAGATGCCAGAAGAGTTTG	GACATCCAGGAGTGCGTGCTTATC
JAM-3	GACTTCTTCCTGCTGCTGCTCTTC	TGGGTTTCGGTTGCTGGATTTGAG
Glut1	GTGACTGGAACACTGGTCCTA	CCAGCCACGTTGCATTGTAG
TNF-α	TCACTGGTGCTCCTGGCTCTG	GCTATCCCTCTTCTCCCGGTCAC
IL-6	CTTCTTGGGACTGATGCTGGTGAC	TCTGTTGGGAGTGGTATCCTCTGTG
IL-1β	CACTACAGGCTCCGAGATGAACAAC	TGTCGTTGCTTGGTTCTCCTTGTAC

qPCR, quantitative Polymerase Chain Reaction; ZO, zonula occludens; JAM, junctional adhesion molecule; Glut1, glucose transporters.

2.13 Statistical Analysis

Data were analysed using Prism 8.0 (GraphPad Software, Boston, MA, USA) and SPSS 23.0 (IBM Corp., Chicago, IL, USA). Results are expressed as mean ± SEM. The *t*-test was used for comparisons between two groups. Pearson correlation analysis (SPSS) assessed associations between changes in RAGE expression and corresponding indicators. A p value < 0.05 was considered statistically significant.

3. Results

3.1 Observation of Clinical Symptoms and Statistics of Blood Glucose Indicators in Mice

Mice in group C remained active, maintained normal diet and water intake, and showed no clinical abnormalities.

Prior to model induction, no significant difference in mean body weight was observed among the three groups of mice ($p > 0.05$). Model induction—achieved through high-sugar, high-fat diet feeding followed by intraperitoneal injection of STZ—was confirmed on day 0 of the experiment. On Day 1, mean body weight in the T0 and T1 groups was significantly higher than that in the control (C) group ($p < 0.05$). Thereafter, mean body weight in the T0 and T1 groups gradually declined over time; by days 7 and 14, the reductions were evident but did not reach statistical significance relative to the C group ($p > 0.05$). By Day 21, mean body weight in the T1 group remained comparable to that in the C group ($p > 0.05$), whereas the T0 group exhibited a statistically significant reduction compared with both the C and T1 groups ($p < 0.05$) (Table 2).

Water intake in the T0 and T1 groups was significantly elevated relative to the control (C) group on Days 1, 7, 14, and 21 of the experiment ($p < 0.05$ or $p < 0.01$). Moreover, water intake in the T1 group was significantly lower than that in the T0 group on Days 7, 14, and 21 ($p < 0.05$) (Fig. 1).

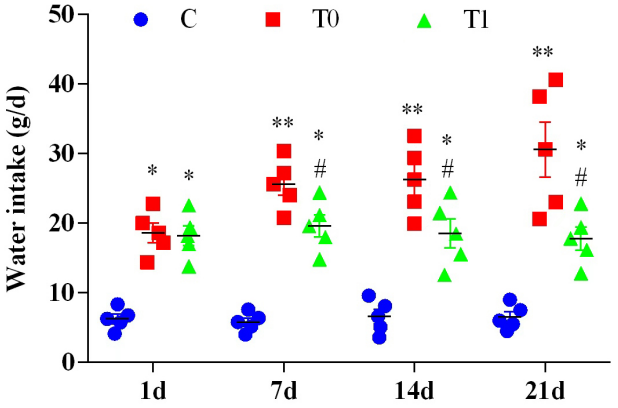

Fig. 1. Comparison of water intake among group C mice, group T0 mice, and group T1 mice (n = 20, the initial total sample size of each group). Note: Compared with group C, * indicates $p < 0.05$, ** indicates $p < 0.01$. Compared with group T0, # indicates $p < 0.05$.

In addition, as the diabetic model progressed, mice in the T0 group exhibited a marked increase in urine output (Fig. 2) and progressive deterioration of coat condition, characterized by unkempt and damp fur (Fig. 3). In contrast, relative to the T0 group, the T1 group showed significantly reduced urine output (Fig. 2), restoration of fur luster and smoothness, and marked improvement in both physical condition and mental alertness (Fig. 3).

At 1, 4, 7, 10, 14, 17 and 21 days, the average blood glucose level of group T0 remained significantly higher than that of group C ($p < 0.01$), and blood glucose in all mice in group T0 exceeded 11.1 mmol/L. With continued TP intervention, blood glucose in group T1 showed a gradual decline compared with group T0. At 10, 14, 17 and 21 days, blood glucose in group T1 was significantly lower than in group T0 ($p < 0.05$) (Table 3).

Table 2. The effect of TP on the body weight of T2DM mice (g), n = 20, initial total sample size of each group.

Group	C	T0	T1
Prior to model establishment	23.38 ± 1.32	23.26 ± 1.04	23.30 ± 1.16
1 d	24.18 ± 1.36	28.60 ± 2.18*	28.70 ± 1.85*
7 d	25.09 ± 1.28	27.82 ± 1.90	27.37 ± 1.56
14 d	26.31 ± 2.06	25.30 ± 1.75	26.80 ± 1.39
21 d	28.06 ± 2.11	23.26 ± 1.35*	26.55 ± 1.32#

Note: Compared with group C, * indicates $p < 0.05$. Compared with group T0, # indicates $p < 0.05$. TP, tea polyphenols; T2DM, type 2 diabetes mellitus; C, control group; T0, diabetes model group; T1, TP-treated group; d, day.

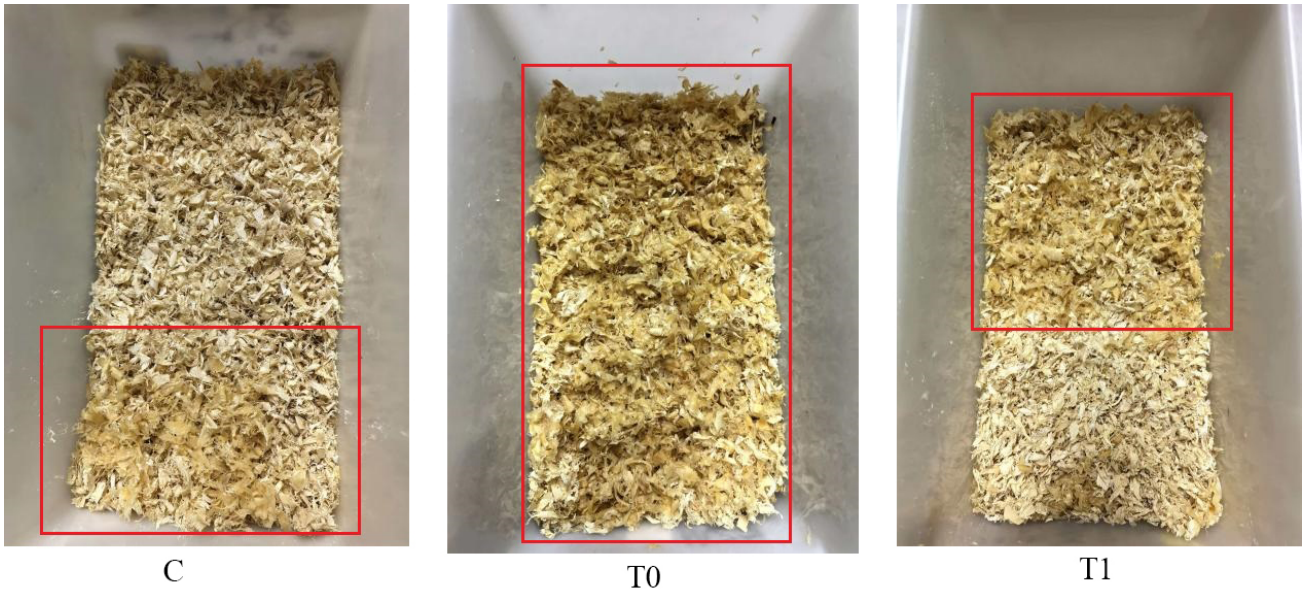

Fig. 2. The effect of TP on bedding of diabetic mice. Note: Compared with group C, the wet area of bedding in group T0 expanded. Compared with group T0, the wet area of bedding in group T1 decreased. The red box indicates the wet area of the bedding.

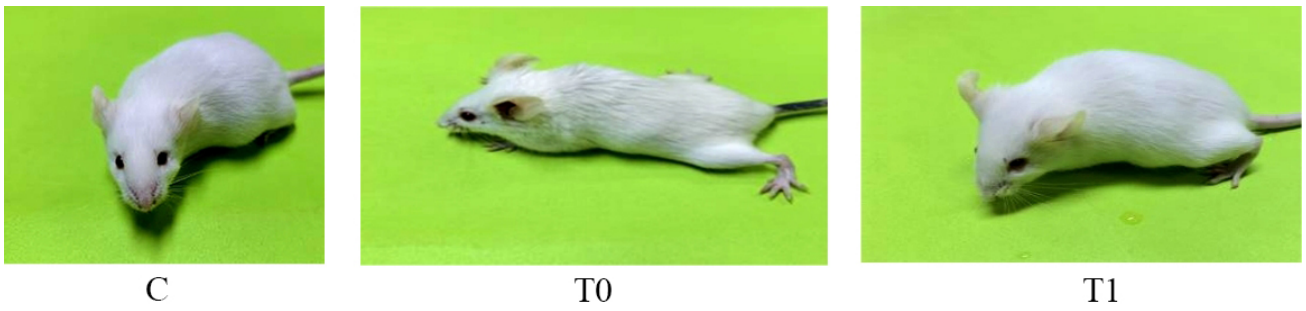

Fig. 3. Comparison of appearance among group C mice, group T0 mice, and group T1 mice at 21 d.

Table 3. Average blood glucose of mice in different treatment groups ($\bar{x} \pm$ SEM, n = 20, initial total sample size of each group).

Groups	1 d	4 d	7 d	10 d	14 d	17 d	21 d
C	6.22 ± 0.72	6.80 ± 0.56	6.70 ± 0.64	6.80 ± 0.58	6.52 ± 0.30	6.55 ± 0.32	6.18 ± 0.46
T0	19.20 ± 0.85**	18.66 ± 0.52**	16.15 ± 0.61**	16.38 ± 0.50**	16.12 ± 0.52**	15.30 ± 0.50**	15.18 ± 0.62**
T1	18.28 ± 0.80	17.41 ± 0.35	15.66 ± 0.22	14.16 ± 0.23#	14.05 ± 0.30#	12.26 ± 0.36#	11.60 ± 0.30#

Note: ** indicates the comparison between group C and group T0, **$p < 0.01$. # indicates the comparison between Group T0 and group T1, # $p < 0.05$.

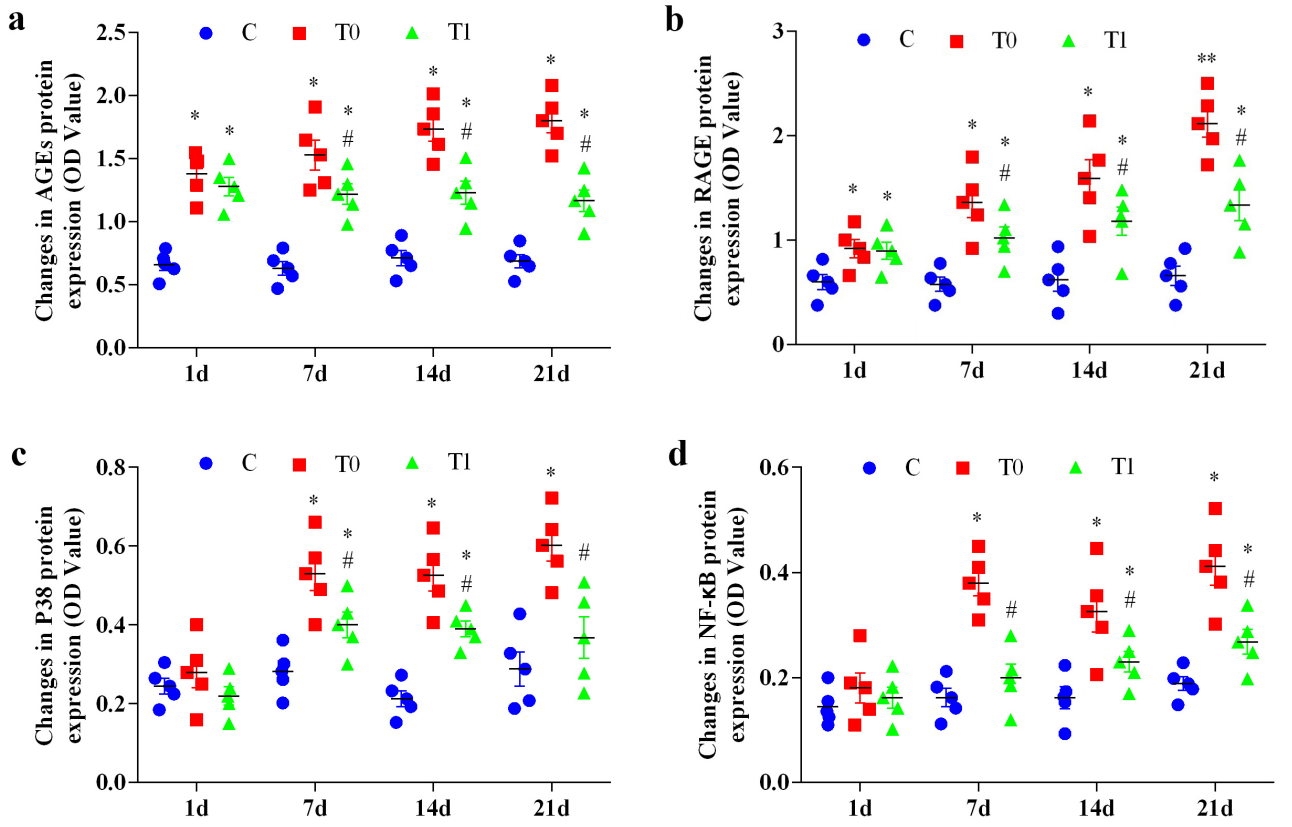

Fig. 4. The effect of TP on the expression of AGEs, RAGE, P38, and NF-κB proteins in the hippocampal tissue of diabetic mice (n = 5). "a" represents the change in AGEs protein expression, "b" represents the change in RAGE protein expression, "c" represents the change in P38 protein expression, and "d" represents the change in NF-κB protein expression. Note: Compared with group C, * indicates $p < 0.05$, and ** indicates $p < 0.01$. Compared with group T0, # indicates $p < 0.05$. AGEs, advanced glycation end products; RAGE, receptor for advanced glycation end products.

3.2 Expression Changes of Key Proteins in the AGEs-RAGE Signaling Pathway

Throughout the experiment, AGEs protein expression in groups T0 and T1 increased significantly compared with group C ($p < 0.05$). At 7, 14 and 21 days, AGEs levels in group T1 were significantly lower than those in group T0 ($p < 0.05$) (Fig. 4a).

RAGE protein expression in groups T0 and T1 increased significantly or highly significantly at 1, 7, 14 and 21 days compared with group C ($p < 0.05$ or $p < 0.01$). At 7, 14 and 21 days, RAGE expression was significantly lower in group T1 than in group T0 ($p < 0.05$) (Fig. 4b).

P38 protein expression increased significantly in group T0 at 7, 14 and 21 days ($p < 0.05$), and in group T1 at 7 and 14 days ($p < 0.05$). At all three time points, P38 expression was significantly lower in group T1 than in group T0 ($p < 0.05$) (Fig. 4c).

Activation of NF-κB increased significantly in group T0 at 7, 14 and 21 days ($p < 0.05$), and in group T1 at 14 and 21 days ($p < 0.05$). At 7, 14 and 21 days, phosphorylation of NF-κB was significantly lower in group T1 than in group T0 ($p < 0.05$) (Fig. 4d).

3.3 Expression Changes of Key Indicators in Inflammation and Oxidative Stress

At day 1, *TNF-α* mRNA expression did not differ significantly among groups ($p > 0.05$). At 7, 14 and 21 days, *TNF-α* mRNA expression increased significantly in both T0 and T1 groups ($p < 0.05$). At 14 and 21 days, expression in group T1 was significantly lower than in group T0 ($p < 0.05$) (Fig. 5a).

Similarly, *IL-6* mRNA expression showed no significant differences at day 1 ($p > 0.05$). At 7, 14 and 21 days, IL-6 expression increased significantly in group T0 ($p < 0.05$), and at 14 and 21 days increased significantly in group T1 ($p < 0.05$). At 21 days, IL-6 expression in group T1 was significantly lower than in group T0 ($p < 0.05$) (Fig. 5b).

For *IL-1β* mRNA, no significant differences were observed at day 1. At 7, 14 and 21 days, IL-1β expression increased significantly in group T0 ($p < 0.05$). At 14 and 21 days, IL-1β expression also increased significantly in group T1 ($p < 0.05$). Moreover, at 14 and 21 days, expression in group T1 was significantly lower than in group T0 ($p < 0.05$) (Fig. 5c).

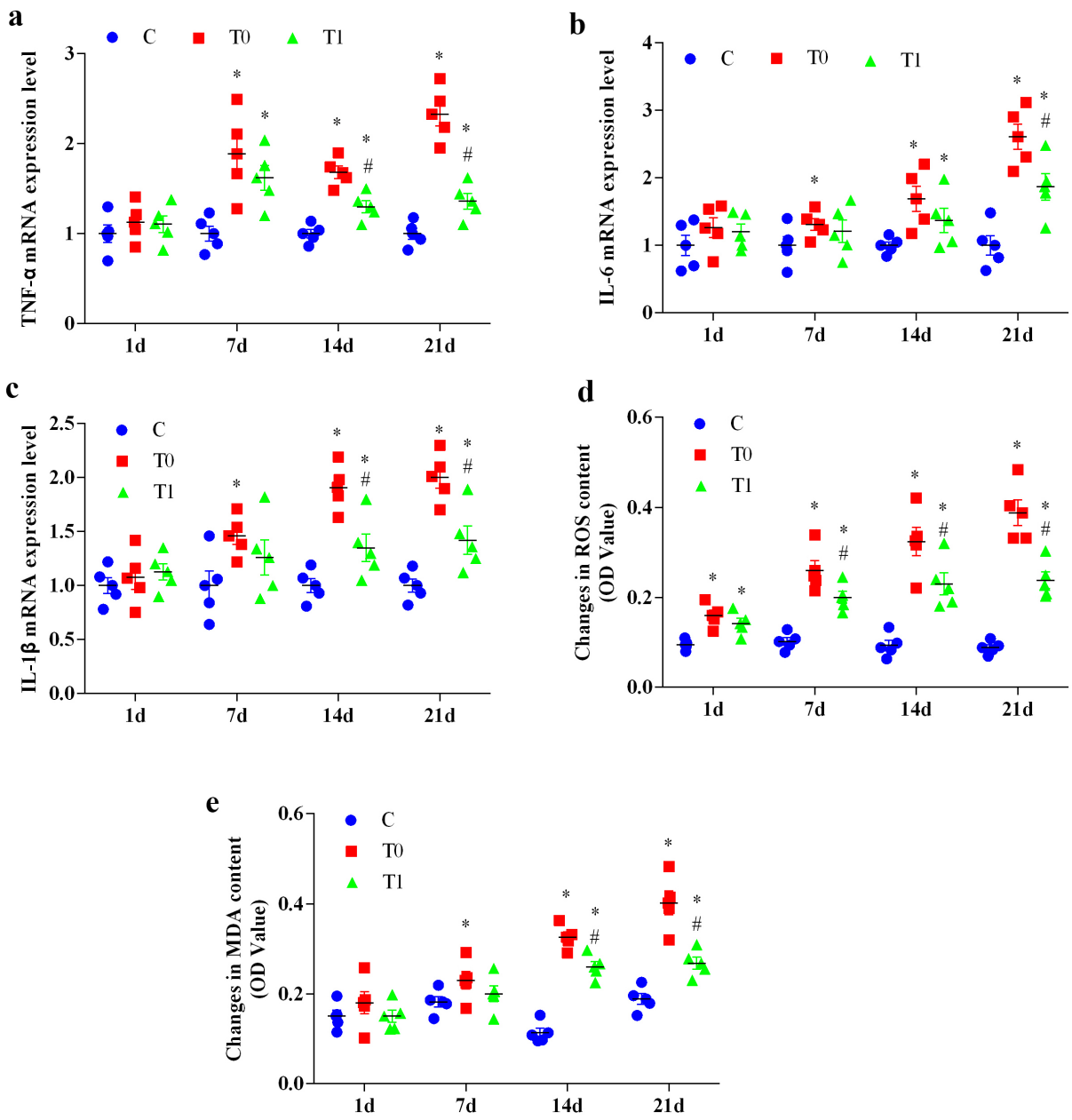

Fig. 5. The effect of TP on the expression changes of key genes in inflammation and oxidative stress in the hippocampal tissue of diabetic mice (n = 5). "a" represents the expression level of *TNF-α* mRNA, "b" represents the expression level of *IL-6* mRNA, "c" represents the expression level of *IL-1β* mRNA, "d" represents the change in ROS content, and "e" represents the change in MDA content. Note: Compared with group C, * indicates $p < 0.05$. Compared with group T0, # indicates $p < 0.05$.

ROS levels were significantly elevated in groups T0 and T1 compared with group C across all time points ($p < 0.05$). At 7, 14 and 21 days, ROS levels in group T1 were significantly lower than in group T0 ($p < 0.05$) (Fig. 5d).

At day 1, MDA levels did not differ significantly among groups. MDA levels increased significantly in group T0 at 7, 14 and 21 days ($p < 0.05$), and in group T1 at 14 and 21 days ($p < 0.05$). At 14 and 21 days, MDA levels were significantly lower in group T1 than in group T0 ($p < 0.05$) (Fig. 5e).

3.4 Expression Changes in Transporter Genes

P-gp protein expression in group T0 showed no significant differences from group C at days 1 and 21 ($p > 0.05$), but increased significantly at 7 and 14 days ($p < 0.05$). In group T1, P-gp levels increased significantly at 7, 14 and 21 days ($p < 0.05$). At 14 and 21 days, P-gp expression was significantly higher in group T1 than in group T0 ($p < 0.05$) (Fig. 6a).

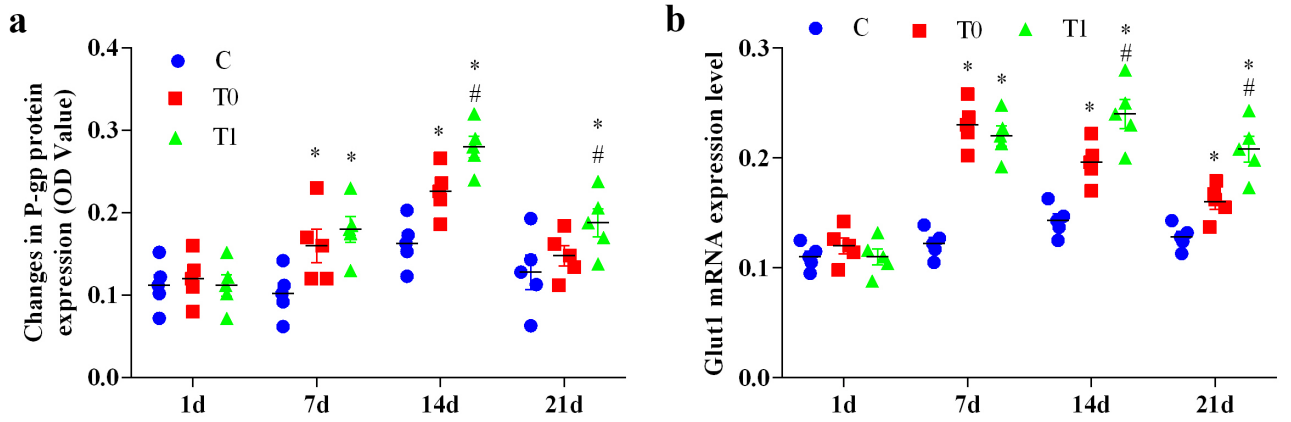

Fig. 6. The effect of TP on P-gp protein expression, and *Glut1* mRNA expression in hippocampal tissue of diabetic mice (n = 5). "a" represents the change in P-gp protein expression, and "b" represents the expression level of *Glut1* mRNA. Note: Compared with group C, * represents $p < 0.05$. Compared with the T0 group, # represents $p < 0.05$. P-gp, P-glycoprotein.

Table 4. Pearson correlation analysis of RAGE and the relevant indicators.

Indicator	P38	NF-κB	IL-6	TNF-α	ROS	Glut1
r value	0.994	0.987	0.992	0.999	0.998	0.960
p value	0.006	0.013	0.008	0.001	0.002	0.040

Glut1 mRNA expression showed no significant differences among groups at day 1 ($p > 0.05$). Expression increased significantly in both T0 and T1 groups at 7, 14 and 21 days ($p < 0.05$). At 14 and 21 days, *Glut1* mRNA expression was significantly higher in group T1 than in group T0 ($p < 0.05$) (Fig. 6b).

3.5 Correlation Analysis

P38, NF-κB, IL-6, TNF-α, ROS and Glut1 are key downstream factors in the AGEs–RAGE signalling pathway. Correlation analysis showed that the expression patterns of these molecules were significantly or highly significantly positively correlated with RAGE protein levels ($p < 0.05$ or $p < 0.01$) (Table 4).

3.6 Expression Changes of Key Genes Closely Related to the BBB

Compared with group C, *Claudin-3* mRNA expression in group T0 increased significantly at 1 and 7 days ($p < 0.05$), showed no significant difference at 14 days, and decreased significantly at 21 days ($p < 0.05$). In group T1, *Claudin-3* mRNA expression increased significantly at 1, 7 and 14 days ($p < 0.05$), but did not differ significantly at 21 days. Compared with group T0, Claudin-3 expression in group T1 was significantly higher at 14 and 21 days ($p < 0.05$) (Fig. 7a).

Claudin-5 mRNA expression in group T0 increased significantly at 1 day ($p < 0.05$), showed no significant difference at 7 days, and decreased significantly at 14 and 21 days ($p < 0.05$). In group T1, *Claudin-5* mRNA expression increased significantly at 1 and 7 days ($p < 0.05$), with no significant differences at 14 and 21 days. Compared with group T0, *Claudin-5* expression in group T1 was significantly higher at 7, 14 and 21 days ($p < 0.05$) (Fig. 7b).

ZO-1 mRNA expression in group T0 did not differ from group C at 1 day but decreased significantly or highly significantly at 7, 14 and 21 days ($p < 0.05$ or $p < 0.01$). Compared with group T0, *ZO-1* expression in group T1 increased significantly at 7, 14 and 21 days ($p < 0.05$) (Fig. 7c).

ZO-3 mRNA expression in group T0 increased significantly at 1 day ($p < 0.05$), showed no significant difference at 7 days, and decreased significantly at 14 and 21 days ($p < 0.05$). In group T1, ZO-3 expression increased significantly at 1 and 7 days ($p < 0.05$). Compared with group T0, *ZO-3* expression in group T1 was significantly higher at 14 and 21 days ($p < 0.05$) (Fig. 7d).

JAM-3 mRNA expression in both T0 and T1 groups increased significantly at 1 day ($p < 0.05$), showed no significant difference at 7 days. Moreover, *JAM-3* mRNA expression in group T0 decreased significantly at 14 and 21 days ($p < 0.05$). Compared with group T0, *JAM-3* expression in group T1 increased significantly at 7, 14 and 21 days ($p < 0.05$) (Fig. 7e).

Occludin mRNA expression in group T0 increased significantly at 1 day ($p < 0.05$), showed no significant difference at 7 and 14 days, and decreased significantly at 21 days ($p < 0.05$). In group T1, Occludin expression increased significantly at 1, 7 and 14 days ($p < 0.05$). Compared with group T0, *Occludin* expression in group T1 was significantly higher at 7, 14 and 21 days ($p < 0.05$) (Fig. 7f).

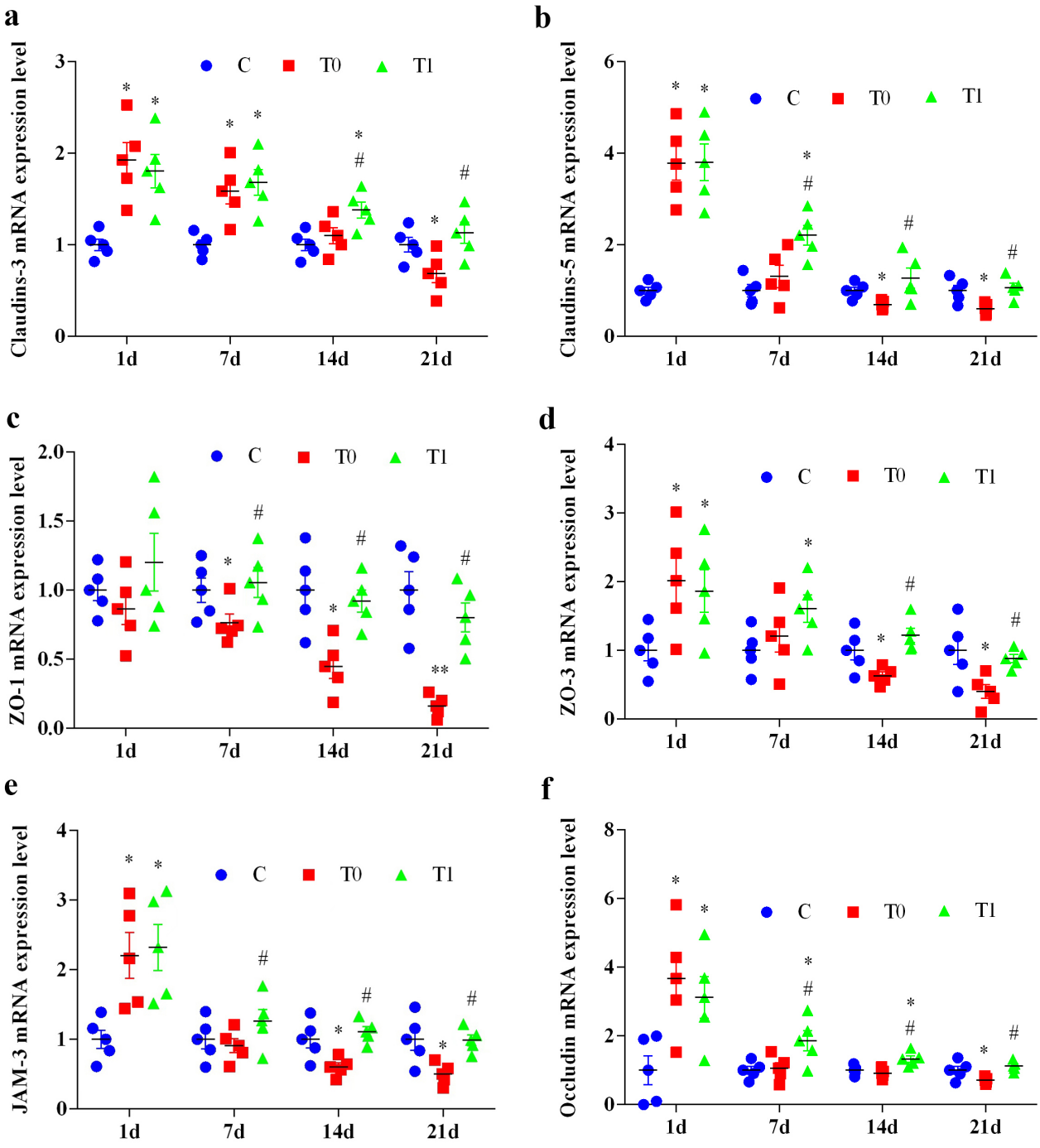

Fig. 7. The effect of TP on the expression level of key molecules of TJ in BBB of diabetic mice (n = 5). "a" represents the expression level of *Claudin-3* mRNA, "b" represents the expression level of *Claudin-5* mRNA, "c" represents the expression level of *ZO-1* mRNA, "d" represents the expression level of *ZO-3* mRNA, "e" represents the expression level of *JAM-3* mRNA, and "f" represents the expression level of *Occludin* mRNA. Note: Compared with group C, * indicates $p < 0.05$. Compared with group T0, ** indicates $p < 0.01$. Compared with group T0, # indicates $p < 0.05$. TJ, tight junction; BBB, blood–brain barrier.

3.7 The Influence of TP on the Histological Structure of the CA1 Region in the Hippocampus of Early Diabetes

H&E staining showed pronounced histological changes in the hippocampus of group T0 compared with group C. Early lesions were observed from CA1 to CA4, with CA1 being most severely affected. At 7 and 14 days, capillary congestion and neuronal structural damage were evident in group T0, with swelling of pyramidal neuron nuclei and cytoplasm. At 21 days, neuronal arrangement became disordered, capillary congestion worsened, and the Virchow–Robin space widened. Some neurons showed lighter cytoplasmic staining and became rounded and

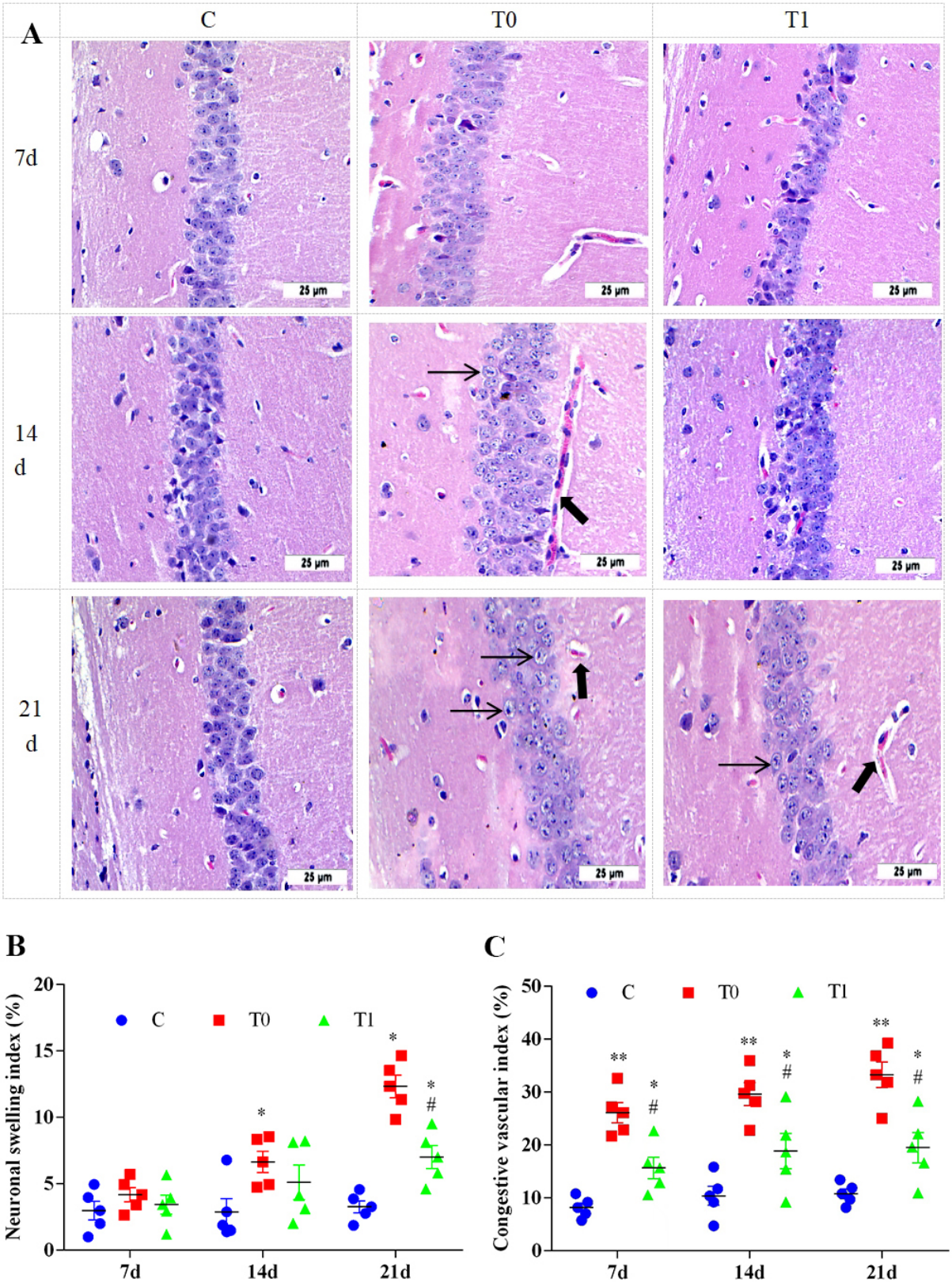

Fig. 8. The effect of TP on the histological structure of the hippocampus in DM mice, n = 5. Note: (A) H&E staining were used to analyze the pathological changes of hippocampal tissue. "➞" indicates that the capillaries were congested and the spaces were enlarged. "➡" indicates the swelling of neurons. (B) Semi-quantitative analysis of neuronal swelling index. (C) Semi-quantitative analysis of vascular congestion index. Compared with group C, * indicates $p < 0.05$, and ** indicates $p < 0.01$. Compared with group T0, # indicates $p < 0.05$. Scale bar = 25 μm. DM, diabetes mellitus.

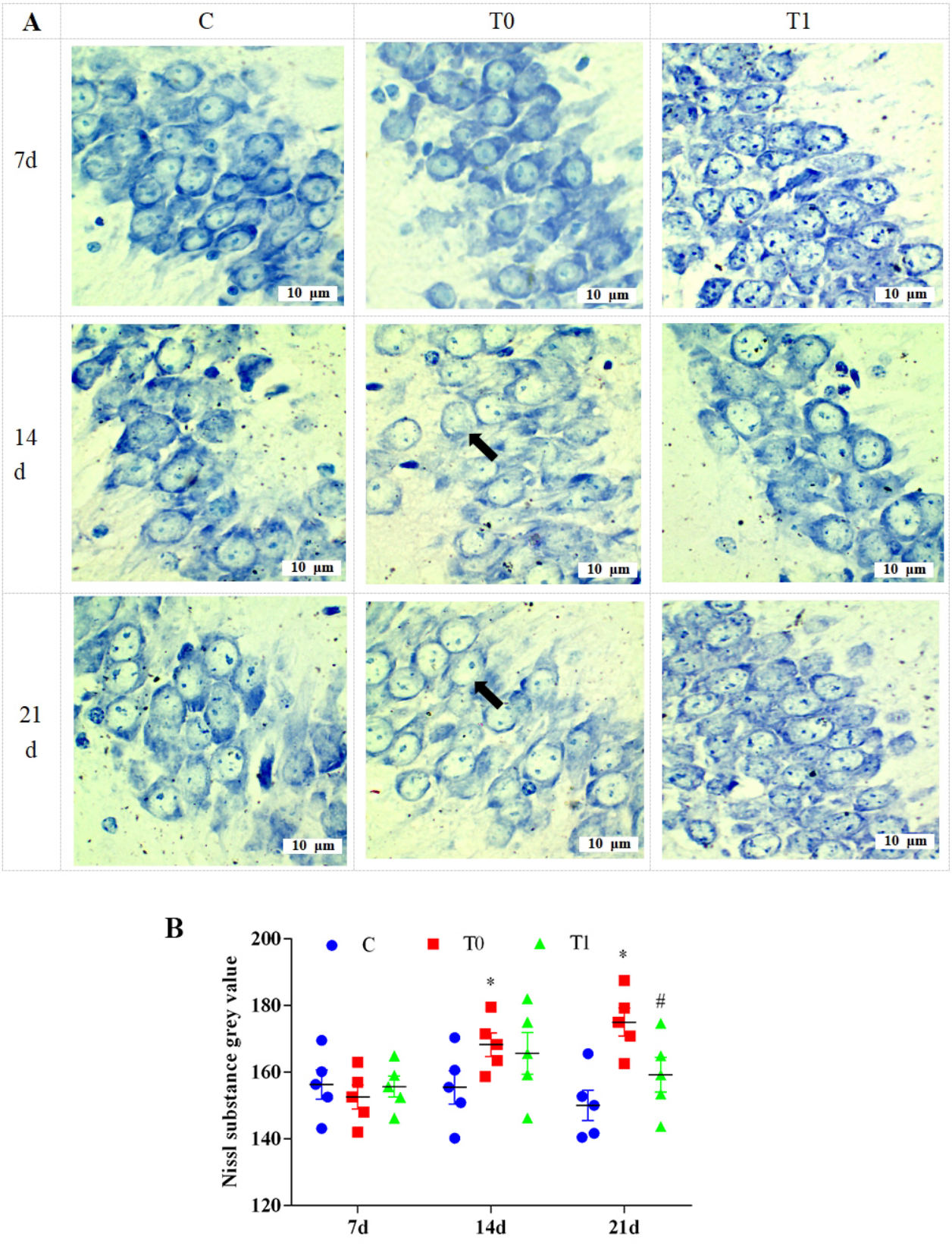

Fig. 9. The effect of TP on the content of Nissl substance in neurons of the CA1 region in the hippocampus of mice, n = 5. Note: (A) Toluidine blue staining. "➡" indicates neurons in which the Nissl substance in the cytoplasm has decreased or disappeared. (B) Semi-quantitative analysis of changes in Nissl substances in neurons. Compared with group C, * indicates $p < 0.05$. Compared with group T0, # indicates $p < 0.05$. Scale bar = 10 μm.

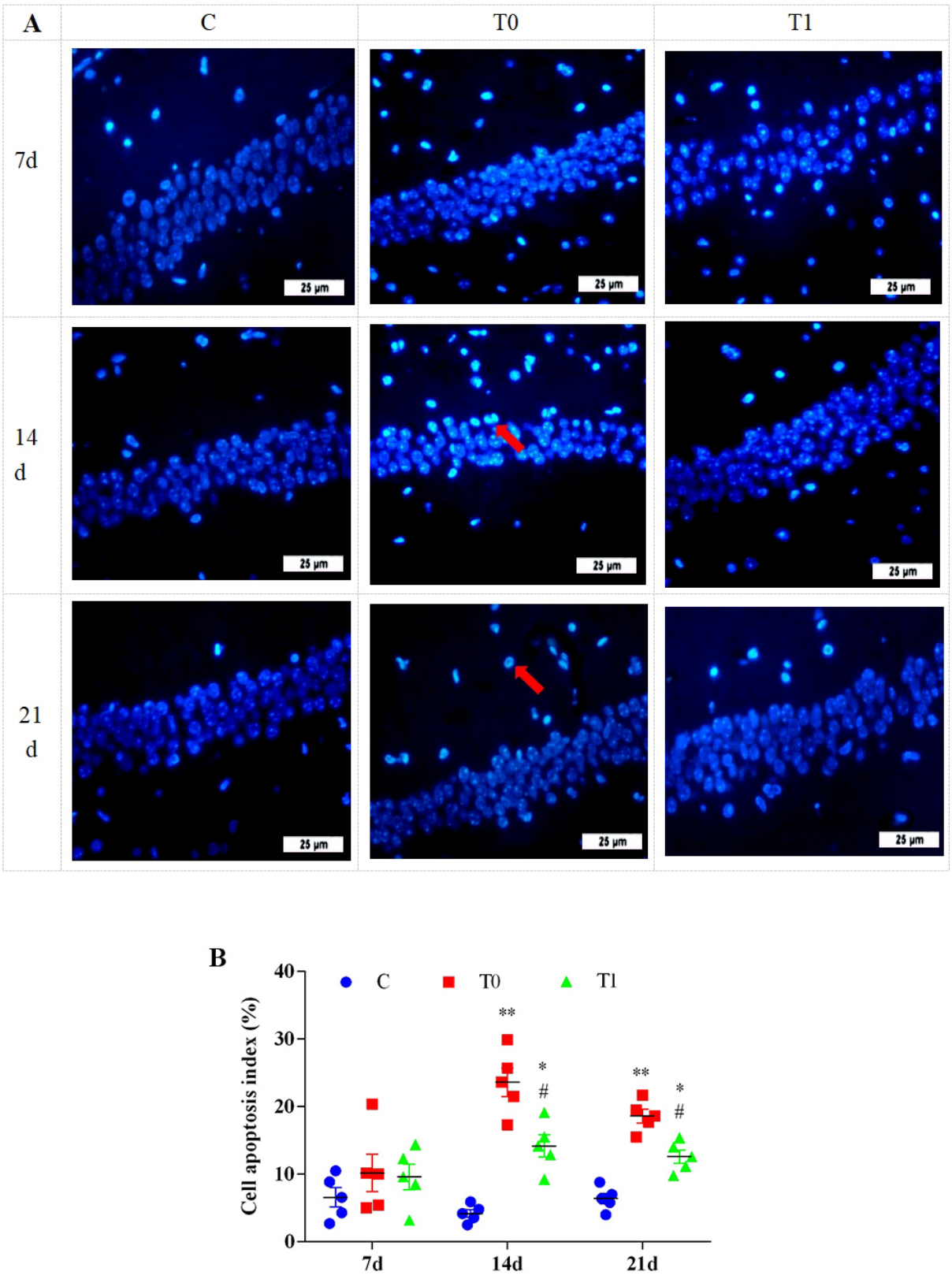

Fig. 10. The effect of TP on apoptosis of hippocampal cells in DM mice, n = 5. Note: (A) Hoechst 33342 staining was used to analyze the pathological changes of hippocampal tissue. "➡" indicates apoptotic cells. (B) Semi-quantitative analysis of apoptotic cells. Compared with group C, * indicates $p < 0.05$, and ** indicates $p < 0.01$. Compared with group T0, # indicates $p < 0.05$. Scale bar = 25 μm.

swollen. In group T1, the Virchow–Robin space was narrower at 21 days, and neuronal swelling was significantly reduced compared with group T0 (Fig. 8A). As shown in Fig. 8B,C, the neuronal swelling index in group T0 increased significantly at 14 and 21 days ($p < 0.05$), and that in group T1 increased significantly at 21 day ($p < 0.05$). In group T1, the index was significantly lower than in group T0 at 21 day ($p < 0.05$). In addition, the congestive vascular index in groups T0 and T1 increased significantly or highly significantly at 7, 14 and 21 days ($p < 0.05$ or $p < 0.01$). Moreover, compared with T0 group, TP treatment significantly reduced this index at 7, 14 and 21 days ($p < 0.05$), indicating that TP reduced neuronal swelling and vascular congestion.

Toluidine blue staining showed no obvious neuronal changes in the CA1 region at 1 and 7 days in group T0. At 14 and 21 days, neurons became rounded and swollen, and Nissl substance decreased significantly. Compared with group T0, Nissl substance in group T1 increased significantly at 14 and 21 days (Fig. 9A). As shown in Fig. 9B, grey values of Nissl substance were significantly higher in group T0 at 14 and 21 days ($p < 0.05$). In group T1, grey values decreased significantly at 21 day compared with group T0 ($p < 0.05$), indicating that TP reduced the loss of Nissl substance in hippocampal neurons.

Hoechst 33342 staining showed no significant differences in apoptotic cells between groups at 1 and 7 days. At 14 and 21 days, apoptotic cells increased significantly in endothelial and glial cells in group T0. In group T1, apoptotic cells in the CA1 region were significantly reduced at both time points (Fig. 10A). As shown in Fig. 10B, the apoptotic index was significantly or highly significantly elevated in groups T0 and T1 at 14 and 21 days ($p < 0.05$ or $p < 0.01$). Moreover, compared with T0 group, TP treatment significantly lowered the apoptotic index at 14 and 21 days ($p < 0.05$), indicating that TP reduced apoptosis in hippocampal tissue of diabetic mice.

4. Discussion

The hippocampus is essential for learning and memory and is highly susceptible to neuronal damage caused by hyperglycaemia, which affects CNS function. The BBB is a cerebrovascular barrier formed by ECs through continuous intercellular TJs, sealing intercellular contact and protecting neurons from circulating factors to maintain a regulated CNS environment. Numerous studies report that persistent hyperglycaemia in diabetes damages the hippocampus, disrupts BBB integrity, and enables harmful circulating substances to enter the brain, leading to neurological complications [19,20].

4.1 The Effect of TP on Clinical Symptoms and FBG in DM Mice

Previous studies show that green tea significantly improves fasting blood glucose, glycosylated haemoglobin and insulin resistance in type II diabetes [21]. Green or black tea alleviates polyuria, polydipsia, hyperglycaemia and other diabetic symptoms in db/db mice by upregulating kidney water reabsorption proteins, including protein kinase C-α (PKC-α), membrane PKC-α and glycosylated UT-A1 [22]. In addition, diabetic model rats exhibit markedly elevated FBG levels; administration of TP at 300 mg/kg significantly reduces FBG [23]. In this study, diabetic mice showed typical symptoms of weight loss, polyuria and polydipsia. After TP administration, these symptoms were substantially alleviated, and FBG was significantly lowered. These findings are consistent with earlier reports [21–23].

4.2 The Effect of TP on the AGEs-RAGE Signalling Pathway in the Hippocampal Tissue of DM Mice

The interaction between AGEs and RAGE contributes to BBB dysfunction. Hyperglycaemia in DM elevates RAGE levels, increases ROS production, activates the NF-κB pathway and promotes the expression of pro-inflammatory mediators, thereby enhancing inflammatory responses [12]. Studies also show that AGEs accumulate in the brains of diabetic rats and induce upregulation of RAGE, creating a cycle of inflammation and oxidative stress that intensifies vascular inflammation [24]. Combined treatment with insulin and idebenone inhibits the ROS/AGE/RAGE/NF-κB signalling pathway, upregulate occludin, claudin-5 and ZO-1, and reduce BBB permeability in diabetic rats, indicating that elevated RAGE may contribute indirectly to BBB injury. Green tea extract reduces the inflammatory response in LPS-stimulated L2 lung epithelial cells during acute respiratory distress syndrome by suppressing NF-κB, NOD-like receptor family, pyrin domain containing 3 (NLRP3), TLR-4 and RAGE expression, as well as IL-12, TNF-α and CRP, while reducing apoptosis and increasing viable cell numbers [25]. EGCG decreases high mobility group box 1 protein (HMGB1) and RAGE expression, inhibits NF-κB activation and reduces neointimal hyperplasia in a rat carotid balloon injury model [26]. In this study, AGEs and RAGE protein levels increased progressively in both diabetic groups, indicating their involvement in early BBB injury. TP administration significantly reduced both proteins. During early hyperglycaemia, changes in P38 and phosphorylated NF-κB expression were not notable; however, both increased under prolonged hyperglycemic conditions. TP significantly reduced P38 and phosphorylated NF-κB, likely through suppression of AGEs and RAGE and subsequent inhibition of downstream effectors [25,26].

4.3 The Effect of TP on the Expression of Oxidative Stress and Inflammatory Genes in the Hippocampal Tissue of DM Mice

Oxidative stress is a physiological response induced by adverse internal or external stimuli. Excessive production of ROS and reactive nitrogen species (RNS) exceeds the body's clearance capacity, disrupts redox homeostasis and leads to an imbalance between oxidative and antioxidative processes. Malondialdehyde (MDA), a final product of lipid peroxidation, is an indicator of lipid peroxidation severity and oxidative stress. Studies report that MDA levels in the hippocampus of type 2 diabetic mice are significantly higher than in normal mice, whereas SOD activity is significantly reduced and inflammatory cytokines such as IL-1β, IL-6, TNF-α and CRP are significantly elevated [11,27]. In male Wistar rats at the prediabetes stage, regular intake of white tea increases lung antioxidant enzyme activity and total antioxidant capacity (TAC) and improves parameters related to protein nitration, lipid peroxidation and histone H2A [28]. In patients with type 2 diabetes, two months of EGCG supplementation (300 mg/d) significantly increases TAC [29]. EGCG also significantly reduces MDA levels in diabetic animal models [30]. In this study, ROS and MDA levels increased significantly in the hippocampal tissues of both diabetic groups throughout the experiment. TP treatment significantly reduced both indicators, suggesting that TP attenuates oxidative stress in diabetic brain tissue, consistent with previous reports [29,30].

Chronic peripheral inflammation induced by persistent hyperglycaemia can activate inflammatory signalling within the CNS, disrupt neuronal structure and function in the hippocampus and contribute to cognitive impairment and behavioural abnormalities. IL-1β, IL-6 and TNF-α are common pro-inflammatory cytokines. Prior studies show that TNF-α, IL-6, IL-1β and MDA levels in the hippocampus of diabetic rats rise significantly compared with nondiabetic control rats ($p < 0.05$) [31]. Other studies report that oxidative stress, inflammatory cytokines and the TXNIP/NLRP3/IL-1β pathway are upregulated in podocytes exposed to high glucose and in diabetic nephropathy mouse kidneys, whereas EGCG reduces ROS and inflammatory factors such as TNF-α, IL-6 and IL-18 [32]. In elderly T2DM model rats, TP (300 mg/kg) regulates intestinal microbiota and inhibits TLR4/NF-κB signalling in the hippocampus, reducing neuroinflammation and improving synaptic plasticity [33]. Curcumin also protects hippocampal tissue in diabetic rats by reducing TNF-α, IL-6, IL-1β and MDA levels [31]. In this study, no significant differences in *TNF-α*, *IL-6* or *IL-1β* mRNA expression were observed at the early stage. With prolonged hyperglycaemia, inflammatory cytokines increased markedly in the diabetes group. Although cytokines also rose in the TP group at later stages, their levels remained significantly lower than in the diabetes group. These results indicate that TP reduces neuroinflammation in the hippocampus, consistent with earlier findings [32,33].

4.4 The Effect of TP on the Expression of Transporter Genes in the Hippocampal Tissue of DM Mice

P-gp is an essential transmembrane transport protein that exports exogenous substances such as drugs and toxins out of cells, thereby influencing drug absorption, distribution and metabolism. In this study, P-gp expression initially increased and then declined during early diabetes. After TP treatment, P-gp expression increased significantly. Early diabetic stress may transiently stimulate P-gp expression as a protective response, consistent with earlier work [10]. As hyperglycaemic injury progressed, P-gp expression declined. TP upregulated P-gp expression, which may enhance the removal of harmful substances and protect brain tissue more effectively.

Glucose transporters (Glut proteins) regulate glucose uptake across membranes. Glut1 is expressed in vascular ECs and astrocytes [34], where it transports glucose across the BBB and into astrocytes for glycolysis. Glut1 has a high affinity for glucose and functions cooperatively with Glut3 to deliver glucose from the CNS interstitial fluid to neurons. Normal Glut1 function is essential for brain glucose uptake and utilisation [35]. Glut1 supports basal glucose uptake, whereas Glut4 mediates insulin-responsive glucose transport in peripheral tissues. Green Tea (GT) and EGCG increase Glut4 expression and reduce insulin resistance [36]. Reduced Glut1 expression impairs glucose transport and utilisation and contributes to brain energy deficiency. *In vivo* studies show that Glut1 levels decrease significantly in the hippocampus of mildly obese type 2 diabetic mice, accompanied by cognitive impairment [37]. *In vitro*, high-glucose exposure decreases Glut1 membrane expression in astrocytes, limiting glucose entry, reducing ATP production and impairing cognitive-related cellular functions [38]. In this study, Glut1 expression increased early in diabetes, then declined as injury progressed. TP treatment significantly increased Glut1 expression. Early diabetic stress may induce compensatory Glut1 expression to improve glucose uptake and mitigate initial metabolic disturbances. As hyperglycaemia persists, *Glut1* expression decreases. TP enhanced *Glut1* mRNA expression, reduced brain tissue damage and supported glucose transport and utilisation, consistent with its effects on Glut4 [35,36].

4.5 The Correlation Between the Expression Changes of RAGE and Downstream Related Factors

In this study, RAGE protein expression exhibited a significant or highly significant positive correlation with P38, NF-κB, IL-6, TNF-α, ROS, and Glut1 expression. These findings suggest that TP may regulate key downstream components of the AGEs–RAGE signalling pathway by suppressing RAGE expression in hippocampal tissue.

4.6 The Effect of TP on the Expression Levels of Key Factors of the BBB in the Hippocampus of DM Mice

Impaired BBB integrity is associated with reduced TJ proteins and inflammation in brain microvessels and neural tissue. Studies show that diabetes-induced PKC activation, overexpression of growth factors and intensified oxidative stress contribute to endothelial dysfunction [39]. EGCG, as a water-soluble compound, reduces Aβ1–42 plaque formation and decreases BBB permeability in ageing rats [40]. A combination of green tea, saffron, trans-resveratrol and phosphatidylcholine improves drug delivery across the BBB, preserves BBB integrity, reduces mitochondrial damage and enhances cell survival in CCF-STTG1 neurodegenerative models. This mixture also modulates cellular energy metabolism and apoptosis and reduces oxidative stress-driven inflammation [41]. GT polyphenols inhibit endothelial hyperpermeability [42]. Several studies also indicate significant reductions in claudin-5, claudin-3, occludin and ZO-1 expression in diabetic mice [43–45], although some T2DM models show increased Occludin and ZO-1 levels. In this study, compared with group C, *ZO-1* mRNA expression showed no significant change at day 1, whereas other related molecules increased significantly. As modeling duration progressed, *claudin-5, claudin-3, occludin, ZO-1, ZO-3* and *JAM-3* mRNA levels decreased significantly, consistent with previous findings [43–45]. TP administration slowed the decline in these TJ molecules. By the end of the experiment, their expression levels in the TP group showed no significant difference from those of the normal group. These observations suggest that early hyperglycaemic stress may promote the production of TJ molecules to counteract BBB injury. However, prolonged hyperglycaemia suppresses TJ molecule production and gradually disrupts BBB structure. TP reduces the long-term effects of hyperglycaemia, promotes TJ molecule expression and alleviates BBB damage [40–42].

4.7 The Effect of TP on the Histological Structure of Hippocampus in DM Mice

Hippocampal tissue consists mainly of neurons (pyramidal and granule cells) and glial cells, forming an extensive synaptic network. STZ-induced DM reduces hippocampal cell proliferation and survival [46]. H&E and Nissl staining reveal neuronal loss in diabetic mice [47]. Previous studies show that apoptosis increases in T2DM and db/db mice [48], with elevated pro-apoptotic proteins and reduced anti-apoptotic and synaptic proteins [49]. EGCG promotes proliferation, migration and angiogenesis of endothelial progenitor cells and inhibits apoptosis [50]. Green tea prevents hippocampal neuronal apoptosis in diabetic rats by inhibiting the JNK/MLCK pathway and improves cognitive function [15]. EGCG also reduces oxidative and nitrosative stress induced by long-term alcohol exposure, increases glutathione (GSH) and enhances antioxidant enzyme activity, improving pathological alterations in the cerebral cortex, cerebellum, and hippocampus [51]. In this study, hippocampal capillaries in group T0 were congested at 7 days. By day 14, cytoplasmic staining became lighter, neurons appeared rounded and swollen, and vascular spaces widened. By day 21, Nissl substance decreased markedly, and apoptosis was increased in glial cells and ECs, consistent with previous studies [48,49]. TP treatment reduced neuronal swelling, narrowed perivascular gaps, lowered apoptosis and increased Nissl substance. These results indicate that hippocampal pathology initiates as early as day 7 after diabetes induction and worsens over time. TP markedly attenuated tissue injury, consistent with earlier findings [15,50,51].

Limitations

This study has several limitations. First, this study was only conducted in early-stage diabetic mice, and the long-term effects of TP on hippocampal structure and BBB integrity remain to be further explored. Second, the protective mechanism was verified mainly at the mRNA and protein expression levels; further in-depth experiments such as gene intervention or pathway blockade are still needed to confirm the causal relationship. Third, this is a preclinical animal study, and the results cannot be directly extrapolated to human clinical applications without further verification.

5. Conclusion

By decreasing the levels of AGEs, RAGE, P38 and phosphorylated NF-κB in the hippocampal tissue of diabetic mice, TP reduced oxidative stress markers (ROS and MDA), suppressed the mRNA expression of pro-inflammatory cytokines (*TNF-*α, *IL-6*, *IL-1*β) and increased P-gp protein expression and *Glut1* mRNA expression. The reduction in inflammation and oxidative stress promoted the expression of key TJ–related genes (*JAM-3*, *ZO-1*, *ZO-3*, *claudin-5*, *claudin-3* and *occludin*), thereby protecting BBB structure. Therefore, TP alleviated capillary congestion and neuronal structural damage in the CA1 region and reduced apoptosis in early-stage diabetic mice. These findings indicate that TP enhances BBB structural integrity by inhibiting the AGE–RAGE signalling pathway and protects hippocampal tissue.

Availability of Data and Materials

The datasets used and/or analyzed during the current study are available from the corresponding author on reasonable request.

Author Contributions

ZX: Conceptualization, data management, formal analysis, investigation, methodology, writing – original draft. YL: Data management, investigation, methodology, validation, writing – original draft. YY: Conceptualization, funding acquisition, project management, supervision, vali-

dation, writing, review and editing. All authors read and approved the final manuscript. All authors have participated sufficiently in the work and agreed to be accountable for all aspects of the work.

Ethics Approval and Consent to Participate

All animal procedures were approved by the Scientific Ethics Committee of Henan Institute of Science and Technology (License No. LLSC2021034). The research was conducted in accordance with the "National Institutes of Health Guidelines for the Care and Use of Laboratory Animals". The research plan has been reviewed and approved by the Institutional Animal Care and Use Committee (IACUC) within the institution.

Acknowledgment

Not applicable.

Funding

This research was supported by the Henan Provincial Science and Technology Research Project (No.232102310480).

Conflict of Interest

The authors declare no conflict of interest.

References

[1] Ziegler D, Porta M, Papanas N, Mota M, Jermendy G, Beltramo E, *et al*. The Role of Biofactors in Diabetic Microvascular Complications. Current Diabetes Reviews. 2022; 18: e250821195830. https://doi.org/10.2174/1871527320666210825112240.

[2] Ye S, Xie DJ, Zhou P, Gao HW, Zhang MT, Chen DB, *et al*. Huang-Pu-Tong-Qiao Formula Ameliorates the Hippocampus Apoptosis in Diabetic Cognitive Dysfunction Mice by Activating CREB/BDNF/TrkB Signaling Pathway. Evidence-based Complementary and Alternative Medicine: ECAM. 2021; 2021: 5514175. https://doi.org/10.1155/2021/5514175.

[3] Alahmari A. Blood-Brain Barrier Overview: Structural and Functional Correlation. Neural Plasticity. 2021; 2021: 6564585. https://doi.org/10.1155/2021/6564585.

[4] Bogush M, Heldt NA, Persidsky Y. Blood Brain Barrier Injury in Diabetes: Unrecognized Effects on Brain and Cognition. Journal of Neuroimmune Pharmacology: the Official Journal of the Society on NeuroImmune Pharmacology. 2017; 12: 593–601. https://doi.org/10.1007/s11481-017-9752-7.

[5] Scalise AA, Kakogiannos N, Zanardi F, Iannelli F, Giannotta M. The blood-brain and gut-vascular barriers: from the perspective of claudins. Tissue Barriers. 2021; 9: 1926190. https://doi.org/10.1080/21688370.2021.1926190.

[6] Profaci CP, Munji RN, Pulido RS, Daneman R. The blood-brain barrier in health and disease: Important unanswered questions. The Journal of Experimental Medicine. 2020; 217: e20190062. https://doi.org/10.1084/jem.20190062.

[7] Yuan S, Liu KJ, Qi Z. Occludin regulation of blood-brain barrier and potential therapeutic target in ischemic stroke. Brain Circulation. 2020; 6: 152–162. https://doi.org/10.4103/bc.bc_29_20.

[8] Kaya M, Ahishali B. Basic physiology of the blood-brain barrier in health and disease: a brief overview. Tissue Barriers. 2021; 9: 1840913. https://doi.org/10.1080/21688370.2020.1840913.

[9] Xu ZY, Fu SX, Zhao HC, Wang YM, Liu Y, Ma JY, *et al*. Dynamic changes in key factors of the blood-brain barrier in early diabetic mice. Journal of Neuropathology and Experimental Neurology. 2024; 83: 763–771. https://doi.org/10.1093/jnen/nlae056.

[10] Prasad S, Sajja RK, Park JH, Naik P, Kaisar MA, Cucullo L. Impact of cigarette smoke extract and hyperglycemic conditions on blood-brain barrier endothelial cells. Fluids and Barriers of the CNS. 2015; 12: 18. https://doi.org/10.1186/s12987-015-0014-x.

[11] Zhu Y, He Y, Yang H, Gao Y, Wang Y, Liu P, *et al*. Semaglutide ameliorates diabetes-associated cognitive dysfunction in mouse model of type 2 diabetes. PloS One. 2025; 20: e0326897. https://doi.org/10.1371/journal.pone.0326897.

[12] Reddy VP, Aryal P, Soni P. RAGE Inhibitors in Neurodegenerative Diseases. Biomedicines. 2023; 11: 1131. https://doi.org/10.3390/biomedicines11041131.

[13] Li X, Cai Y, Zhang Z, Zhou J. Glial and Vascular Cell Regulation of the Blood-Brain Barrier in Diabetes. Diabetes & Metabolism Journal. 2022; 46: 222–238. https://doi.org/10.4093/dmj.2021.0146.

[14] Chen TS, Liou SY, Lin HH, Hung MY, Lin CC, Lin YM, *et al*. Oral administration of green tea Epigallocatechin-3-gallate reduces oxidative stress and enhances restoration of cardiac function in diabetic rats receiving autologous transplantation of adipose-derived stem cells. Archives of Physiology and Biochemistry. 2021; 127: 82–89. https://doi.org/10.1080/13813455.2019.1614631.

[15] Xu Y, Liu S, Zhu L, Dai L, Qian W, Zhang J, *et al*. Green tea protects against hippocampal neuronal apoptosis in diabetic encephalopathy by inhibiting JNK/MLCK signaling. Molecular Medicine Reports. 2021; 24: 575. https://doi.org/10.3892/mmr.2021.12214.

[16] Zhao SY, Zhao HH, Hao TT, Li WW, Guo H. Effect of Bushen Huoxue Prescription on Cognitive Dysfunction of KK-Ay Type 2 Diabetic Mice. Evidence-based Complementary and Alternative Medicine: ECAM. 2021; 2021: 6656362. https://doi.org/10.1155/2021/6656362.

[17] Chhipa AS, Borse SP, Baksi R, Lalotra S, Nivsarkar M. Targeting receptors of advanced glycation end products (RAGE): Preventing diabetes induced cancer and diabetic complications. Pathology, Research and Practice. 2019; 215: 152643. https://doi.org/10.1016/j.prp.2019.152643.

[18] Hou B, Qiang G, Zhao Y, Yang X, Chen X, Yan Y, *et al*. Salvianolic Acid A Protects Against Diabetic Nephropathy through Ameliorating Glomerular Endothelial Dysfunction via Inhibiting AGE-RAGE Signaling. Cellular Physiology and Biochemistry: International Journal of Experimental Cellular Physiology, Biochemistry, and Pharmacology. 2017; 44: 2378–2394. https://doi.org/10.1159/000486154.

[19] Kook SY, Hong HS, Moon M, Ha CM, Chang S, Mook-Jung I. Aβ_{1-42}-RAGE interaction disrupts tight junctions of the blood-brain barrier via Ca^{2+}-calcineurin signaling. The Journal of Neuroscience: the Official Journal of the Society for Neuroscience. 2012; 32: 8845–8854. https://doi.org/10.1523/JNEUROSCI.6102-11.2012.

[20] Vargas-Soria M, García-Alloza M, Corraliza-Gómez M. Effects of Diabetes on Microglial Physiology: a Systematic Review of in Vitro, Preclinical and Clinical Studies. Journal of Neuroinflammation. 2023; 20: 57. https://doi:10.1186/s12974-023-02740-x.

[21] Jia MJ, Liu XN, Liang YC, Liu DL, Li HL. The effect of green tea on patients with type 2 diabetes mellitus: A meta-

analysis. Medicine. 2024; 103: e39702. https://doi.org/10.1097/MD.0000000000039702.

[22] Zhao G, Yang L, Ge Y, Qiu Z, Tang D, Fang Y, *et al*. Tea drinking effectively improves symptoms of diabetes and prevents hepatorenal damage in mice. Food Research International (Ottawa, Ont.). 2025; 211: 116502. https://doi.org/10.1016/j.foodres.2025.116502.

[23] Xie H, Feng W, Wang X, Chen S, Cheng L, Lyu C, *et al*. Tea polyphenols improves depression-like behavior in aged type 2diabetes rats by regulating microglia polarization. Wei Sheng Yan Jiu = Journal of Hygiene Research. 2024; 53: 71–87. https://doi.org/10.19813/j.cnki.weishengyanjiu.2024.01.011.

[24] Delrue C, Speeckaert R, Delanghe JR, Speeckaert MM. The Potential Influence of Advanced Glycation End Products and (s)RAGE in Rheumatic Diseases. International Journal of Molecular Sciences. 2023; 24: 2894. https://doi.org/10.3390/ijms24032894.

[25] Priyandoko D, Widowati W, Lenny L, Novianti S, Revika R, Kusuma HSW, *et al*. Green Tea Extract Reduced Lipopolysaccharide-Induced Inflammation in L2 Cells as Acute Respiratory Distress Syndrome Model Through Genes and Cytokine Pro-Inflammatory. Avicenna Journal of Medical Biotechnology. 2024; 16: 57–65. https://doi.org/10.18502/ajmb.v16i1.14172.

[26] Yang B, Gao P, Wu X, Yu J, Li Y, Meng R, *et al*. Epigallocatechin-3-gallate attenuates neointimal hyperplasia in a rat model of carotid artery injury by inhibition of high mobility group box 1 expression. Experimental and Therapeutic Medicine. 2017; 14: 1975–1982. https://doi.org/10.3892/etm.2017.4774.

[27] Gupta M, Rumman M, Singh B, Pandey S. Protective effects of berberine against diabetes-associated cognitive decline in mice. Acta Diabetologica. 2025; 62: 943–955. https://doi.org/10.1007/s00592-024-02411-0.

[28] Silveira AC, Rato L, Oliveira PF, Alves MG, Silva BM. White Tea Intake Abrogates Markers of Streptozotocin-Induced Prediabetes Oxidative Stress in Rat Lungs'. Molecules (Basel, Switzerland). 2021; 26: 3894. https://doi.org/10.3390/molecules26133894.

[29] Wan C, Ouyang J, Li M, Rengasamy KRR, Liu Z. Effects of green tea polyphenol extract and epigallocatechin-3-O-gallate on diabetes mellitus and diabetic complications: Recent advances. Critical Reviews in Food Science and Nutrition. 2024; 64: 5719–5747. https://doi.org/10.1080/10408398.2022.2157372.

[30] Li W, Zhu C, Liu T, Zhang W, Liu X, Li P, *et al*. Epigallocatechin-3-gallate ameliorates glucolipid metabolism and oxidative stress in type 2 diabetic rats. Diabetes & Vascular Disease Research. 2020; 17: 1479164120966998. https://doi.org/10.1177/1479164120966998.

[31] Özsan M, Saygili Düzova Ü, Dönmez N. Neuroprotective role of curcumin on the hippocampus against the oxidative stress and inflammation of streptozotocin-induced diabetes in rats. Metabolic Brain Disease. 2024; 40: 24. https://doi.org/10.1007/s11011-024-01438-0.

[32] Wang Y, Wang Q, Wang M, Wang X, Liu Q, Lv S, *et al*. Epigallocatechin-3-Gallate Ameliorates Diabetic Kidney Disease by Inhibiting the TXNIP/NLRP3/IL-1β Signaling Pathway. Food Science & Nutrition. 2024; 12: 10800–10815. https://doi.org/10.1002/fsn3.4617.

[33] Lv C, Cheng L, Feng W, Xie H, Kou J, Wang L, *et al*. Targeting microbiota-immune-synaptic plasticity to explore the effect of tea polyphenols on improving memory in the aged type 2 diabetic rat model. Nutritional Neuroscience. 2024; 27: 1422–1438. https://doi.org/10.1080/1028415X.2024.2341188.

[34] Cornford EM, Hyman S. Localization of brain endothelial luminal and abluminal transporters with immunogold electron microscopy. NeuroRx: the Journal of the American Society for Experimental NeuroTherapeutics. 2005; 2: 27–43. https://doi.org/10.1602/neurorx.2.1.27.

[35] Koepsell H. Glucose transporters in brain in health and disease. Pflugers Archiv: European Journal of Physiology. 2020; 472: 1299–1343. https://doi.org/10.1007/s00424-020-02441-x.

[36] Yan J, Zhao Y, Suo S, Liu Y, Zhao B. Green tea catechins ameliorate adipose insulin resistance by improving oxidative stress. Free Radical Biology & Medicine. 2012; 52: 1648–1657. https://doi.org/10.1016/j.freeradbiomed.2012.01.033.

[37] Liang Y, Luo S, Wan EYF, Cheung CL, Gill D, Au Yeung SL. Relative effects of genetically proxied glucagon-like peptide-1 receptor agonism on muscle and fat mass: A Mendelian randomization study. Diabetes, Obesity & Metabolism. 2025; 27: 2280–2283. https://doi.org/10.1111/dom.16171.

[38] Thieren L, Zanker HS, Droux J, Dalvi U, Wyss MT, Waag R, *et al*. Astrocytic GLUT1 deletion in adult mice enhances glucose metabolism and resilience to stroke. Nature Communications. 2025; 16: 4190. https://doi.org/10.1038/s41467-025-59400-2.

[39] Calles-Escandon J, Cipolla M. Diabetes and endothelial dysfunction: a clinical perspective. Endocrine Reviews. 2001; 22: 36–52. https://doi.org/10.1210/edrv.22.1.0417.

[40] Wei BB, Liu MY, Zhong X, Yao WF, Wei MJ. Increased BBB permeability contributes to EGCG-caused cognitive function improvement in natural aging rats: pharmacokinetic and distribution analyses. Acta Pharmacologica Sinica. 2019; 40: 1490–1500. https://doi.org/10.1038/s41401-019-0243-7.

[41] Mulè S, Ferrari S, Rosso G, Galla R, Battaglia S, Curti V, *et al*. The Combined Effect of Green Tea, Saffron, Resveratrol, and Citicoline against Neurodegeneration Induced by Oxidative Stress in an *In Vitro* Model of Cognitive Decline. Oxidative Medicine and Cellular Longevity. 2024; 2024: 7465045. https://doi.org/10.1155/2024/7465045.

[42] Zuo X, Tian C, Zhao N, Ren W, Meng Y, Jin X, *et al*. Tea polyphenols alleviate high fat and high glucose-induced endothelial hyperpermeability by attenuating ROS production via NADPH oxidase pathway. BMC Research Notes. 2014; 7: 120. https://doi.org/10.1186/1756-0500-7-120.

[43] Zhao Q, Zhang F, Yu Z, Guo S, Liu N, Jiang Y, *et al*. HDAC3 inhibition prevents blood-brain barrier permeability through Nrf2 activation in type 2 diabetes male mice. Journal of Neuroinflammation. 2019; 16: 103. https://doi.org/10.1186/s12974-019-1495-3.

[44] Yang B, Li Y, Ma Y, Zhang X, Yang L, Shen X, *et al*. Selenium attenuates ischemia/reperfusion injury-induced damage to the blood-brain barrier in hyperglycemia through PI3K/AKT/mTOR pathway-mediated autophagy inhibition. International Journal of Molecular Medicine. 2021; 48: 178. https://doi.org/10.3892/ijmm.2021.5011.

[45] Muneeb M, Mansou SM, Saleh S, Mohammed RA. Vitamin D and rosuvastatin alleviate type-II diabetes-induced cognitive dysfunction by modulating neuroinflammation and canonical/noncanonical Wnt/β-catenin signaling. PloS One. 2022; 17: e0277457. https://doi.org/10.1371/journal.pone.0277457.

[46] Ho N, Sommers MS, Lucki I. Effects of diabetes on hippocampal neurogenesis: links to cognition and depression. Neuroscience and Biobehavioral Reviews. 2013; 37: 1346–1362. https://doi.org/10.1016/j.neubiorev.2013.03.010.

[47] Nan X, Sun Q, Xu X, Yang Y, Zhen Y, Zhang Y, *et al*. Forsythoside B ameliorates diabetic cognitive dysfunction by inhibiting hippocampal neuroinflammation and reducing synaptic dysfunction in ovariectomized mice. Frontiers in Aging Neuroscience. 2022; 14: 974690. https://doi.org/10.3389/fnagi.2022.974690.

[48] Xu Y, Cao K, Guo B, Xiang J, Dong YT, Qi XL, *et al*. Lowered

levels of nicotinic acetylcholine receptors and elevated apoptosis in the hippocampus of brains from patients with type 2 diabetes mellitus and *db/db* mice. Aging. 2020; 12: 14205–14218. https://doi.org/10.18632/aging.103435.

[49] Rom S, Heldt NA, Gajghate S, Seliga A, Reichenbach NL, Persidsky Y. Hyperglycemia and advanced glycation end products disrupt BBB and promote occludin and claudin-5 protein secretion on extracellular microvesicles. Scientific Reports. 2020; 10: 7274. https://doi.org/10.1038/s41598-020-64349-x.

[50] Li D, Mao Y, Zhang X, Wang Y, Tang H, Huang H, *et al*. Epigallocatechin-3-Gallate Promotes Recanalization in Deep Vein Thrombosis by Modulating Endothelial Progenitor Cell Ferroptosis Through the Nrf2 Pathway. Phytotherapy Research: PTR. 2025; 39: 1632–1644. https://doi.org/10.1002/ptr.8457.

[51] Kodidela S, Shaik FB, Mittameedi CM, Mugudeeswaran S. Influence of green tea on alcohol aggravated neurodegeneration of cortex, cerebellum and hippocampus of STZ-induced diabetic rats. Heliyon. 2023; 9: e17385. https://doi.org/10.1016/j.heliyon.2023.e17385.